Modeling Human Open-loop Tracking Behavior

Paul. R. Davidson[1,*] , Richard. D. Jones[1,2,3], John. H. Andreae[1], Harsha. R. Sirisena[1]
[1] Electrical and Electronic Engineering, University of Canterbury, Christchurch, New Zealand
[2] Medical Physics and Bioengineering, Christchurch Hospital, Christchurch, New Zealand
[3] Medicine, Christchurch School of Medicine, University of Otago, Christchurch, New Zealand

***Abstract*—A nonlinear generalization of the Adaptive Model Theory, nAMT, is compared with human open-loop tracking data across the same range of conditions. The resulting simulations produced effects that mirrored the closed- and open-loop characteristics of the experimental response trajectories. This supports the use of an internal feedback loop for the inversion of external systems in the nAMT model. Other control-systems models (both AMT and feedback-error learning) were unable to reproduce the observed disparity between closed- and open-loop results without fundamental modification. A low internal feedback loop-gain, incorporating a substantial derivative component, caused this effect. This low gain produced acceptable performance due to the relatively low target bandwidth used in the study, allowing the feedback control component to function. Maintenance of the loop-gain at the lowest possible levels is thought to maximize the internal stability of the inverse. The simulation work confirmed that the nAMT model is capable of reproducing human behavior under a wide range of conditions.**

***Keywords*—Internal models, motor learning, adaptive inverse control, motor control modelling, tracking task**

I. Introduction

IN a recent experimental study [1], human open-loop tracking data was obtained. This study revealed unexpected open-loop response characteristics (obtained by response cursor blanking) which could not be explained by existing adaptive control systems human motor control models such as Feedback Error Learning (FEL) [2-4] or Adaptive Model (AMT) [5, 6]. A new human motor control model, developed as a nonlinear generalization of AMT, exhibits open-loop behaviour differing from these models. This generalization, called nonlinear AMT (nAMT), was used to simulate the experimental open-loop tracking data with the aim of explaining the open-loop spectral characteristics.

II. Primary Features of Experimental Results

The tracking study reported in [1] produced response trajectories exhibiting unusual characteristics, particularly when the subjects were deprived of response feedback. The primary features of the spectral characteristics of the response trajectories are summarized here and represented graphically in the results section (see Fig. 3 and Fig. 5).

The open-loop responses for all controlled systems showed a mean high-pass gain with a cutoff frequency of approximately 0.3 Hz. This attenuation of low frequencies was unexpected. The mean open-loop phase responses exhibited a phase lead relative to the mean closed-loop phase. This phase lead effect was much stronger for the nonlinear static system, which exhibited an open-loop phase lead peaking at 15–20°. The dynamic linear system also showed a mean phase lead from 0–3 Hz which was absent in closed-loop. The open-loop results also exhibited a characteristic low-frequency drop in mean coherence.

The open-loop results do not suggest that the human subjects are attempting to reach a transfer function of unity, representing accurate tracking (as has been observed for closed-loop tracking). In fact, a quite different relationship between target and response appears to have emerged.

In contrast, the closed-loop gain was close to unity (as expected for the human operator after extensive training) across the target bandwidth. No attenuation of low frequencies was evident. The mean phase responses were close to zero, except for the dynamic linear system which exhibited uncompensated phase lag. The mean closed-loop coherence was very close to unity for all three systems, indicating relatively little noise or nonlinearity.

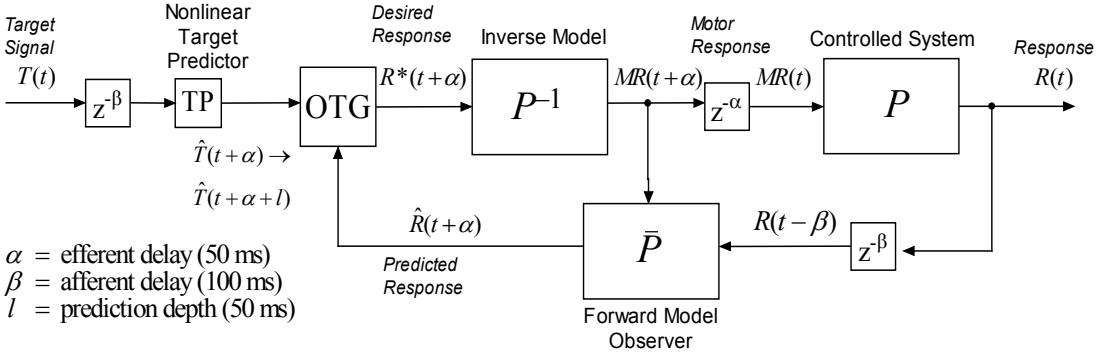

Fig. 1. nAMT model structure used in simulations.

* p.davidson@ieee.org

Report Documentation Page

Report Date	Report Type	Dates Covered (from... to)
25 Oct 2001	N/A	-

Title and Subtitle Modeling Human Open-Loop Tracking Behavior	**Contract Number**
	Grant Number
	Program Element Number
Author(s)	**Project Number**
	Task Number
	Work Unit Number
Performing Organization Name(s) and Address(es) Electrical and Electronic Engineering University of Canterbury Christchurch, New Zealand	**Performing Organization Report Number**
Sponsoring/Monitoring Agency Name(s) and Address(es) US Army Research, Development & Standardization Group (UK) PSC 802 Box 15 FPO AE 09499-1500	**Sponsor/Monitor's Acronym(s)**
	Sponsor/Monitor's Report Number(s)

Distribution/Availability Statement
Approved for public release, distribution unlimited

Supplementary Notes
Papers from 23rd Annual International Conference of the IEEE Engineering in Medicine and Biology Society, October 25-28, 2001, held in Istanbul, Turkey. See also ADM001351 for entire conference on cd-rom.

Abstract

Subject Terms

Report Classification unclassified	**Classification of this page** unclassified
Classification of Abstract unclassified	**Limitation of Abstract** UU

Number of Pages
4

III. Methodology

A. Unblanked Simulation Structure

The model structure shown in Fig. 1 was used in the closed-loop training phase of all simulations. The inverse model is formed by placing the forward model into a high-gain internal-feedback loop [7-9]. In this model, the musculoskeletal system is considered to be perfectly compensated for (since the experimental results were recorded after substantial zero-order practice) and is therefore absent from the diagram. The target signal *T(t)* and the external system *P* were taken directly from the experimental study. The remaining model parameters were initialized with typical parameters for a normal individual [10].

B. Blanked Simulation Structure

Response cursor blanking was simulated by removing response feedback $R(t)$ from the model shown in Fig. 1. It is unclear exactly how the nervous system compensates for the loss of this feedback signal and how best to represent this compensation in the model.

The most efficient course of action would likely involve replacing *R(t)* with the most accurate internal estimate of that signal. *R(t)* can be replaced at two places in Fig. 1: immediately after sensory feedback reaches brain $R(t-\beta)$, or immediately prior to reaching the response planner (called the Optimum Trajectory Generator, or OTG in AMT) at $\hat{R}(t+\alpha)$. Investigation revealed that replacing $\hat{R}(t+\alpha)$ with $R^*(t+\alpha)$ produced the results most consistent with experimental data (see Fig. 2), which is equivalent to suspending corrective action during open-loop control.

IV. Simulation Procedure

A. Dynamic Linear External System Simulation

Simulation of the experimental runs began with the dynamic linear external system used by Group A in the experiment (3rd order Chebyshev Type I low-pass filter with cutoff frequency of 3 Hz). Fifteen runs were simulated in accordance with the 15 experimental runs performed by the human subjects. The model was initialized with several different adaptation coefficients μ so that an appropriate learning rate could be determined. μ = 0.001 produced a response with an appropriate closed-loop learning time constant (compared with experimental results from human subjects) and these results are therefore reported.

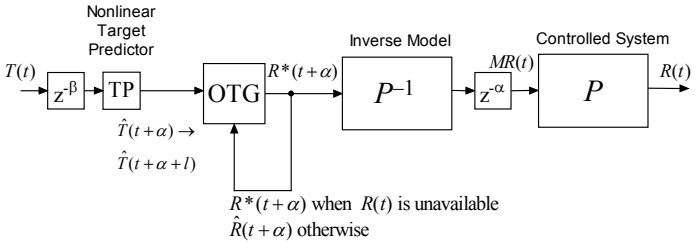

Fig. 2. Open-loop Structure 1. Approach based on suspending corrective action.

The internal feedback loop gain *K*, used to invert the forward model, was defined as

$$K(e) = Pe + I\int e.dt + D\frac{de}{dt},$$

where e is the feedback loop error.

The internal feedback loop-gain parameters previously found to produce good results for a zero-order system were used for these runs ($P = 0.5$, $D = 1$, $I = 0.05$). Trial runs with various other feedback-loop gains produced no clear improvements, and it was very desirable to maintain similar settings between external systems.

B. Static Nonlinear External System Simulation

For consistency, exactly the same experimental procedure and model parameters used for the dynamic linear system were used in this simulation. The external system was as used for Group B in the experiment defined by

$$f(\theta) = 312\left(6\left(\frac{\theta}{180}\text{-}0.4\right)^3 + 0.2\left(\frac{\theta}{180}\text{-}0.4\right) + 0.474\right)$$

where θ is the steering wheel input angle (in deg).

C. Analysis

A full quasi-linear analysis using the correlation method [11] was performed, in which the transfer function and coherence functions were calculated. The remnant power function was represented by calculating the coherence function (which specifies essentially the same information). Spectral estimates were calculated at 6 frequencies within the target bandwidth of 0.6 Hz, providing a frequency resolution of 0.1 Hz.

V. Results

A. Dynamic Linear System

The transfer function and coherence plots for the final run (run 15) are shown in Fig. 3. The closed-loop results show a phase lag and a gain above 0.9 at all frequencies. The coherence is also very high in closed-loop. These superior closed-loop results are due to the action of the feedback controller. The experimental results exhibit less coherence and more variance than the simulation, which was expected because noise was not included in the simulation.

The open-loop results show the same characteristic drop in gain and coherence below 0.3 Hz as was observed in the experimental results. The open-loop results also show a phase lead consistent with the results of several individual subjects, though this effect is obscured in the mean.

By the final run, the simulated open-loop trajectory exhibits characteristics visually similar to the mean response trajectories of the experimental subjects (Fig. 4). The simulated trajectory remains within one standard deviation of

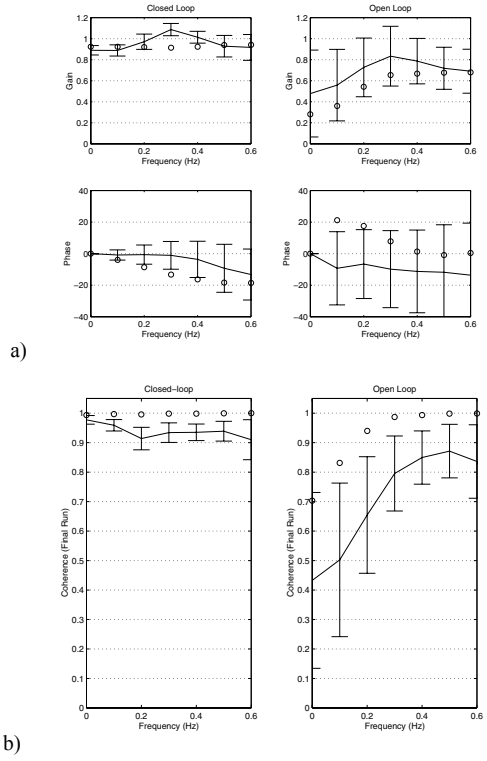

Fig. 3. Simulated a) transfer function and b) coherence for dynamic linear external system after 15 runs. Bars indicate standard deviation. Mean experimental results (final run) shown with solid lines. Bars indicate sd. Simulated results indicated with circles.

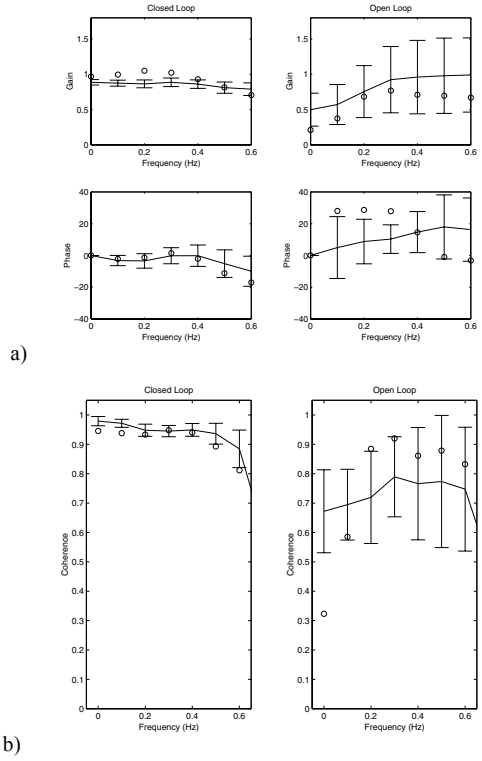

Fig. 5. Simulated a) transfer function and b) coherence for static nonlinear external system after 15 runs. Bars indicate standard deviation. Mean experimental results (final run) shown with solid lines. Bars indicate sd. Simulated results indicated with circles.

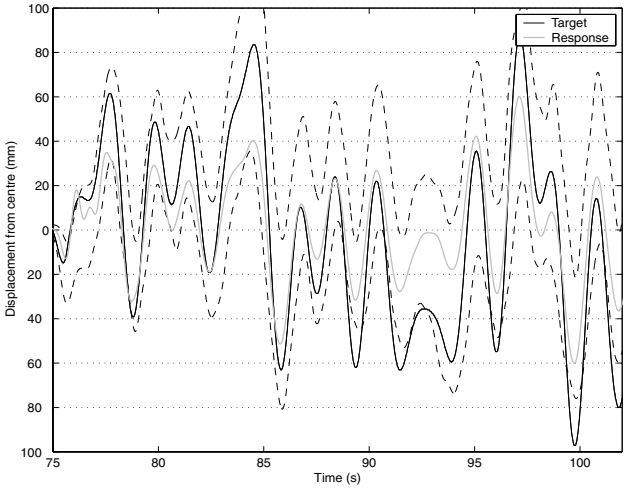

Fig. 4. Simulated open-loop response after 15 runs (dynamic linear system). Dashed lines indicate experimental sd.

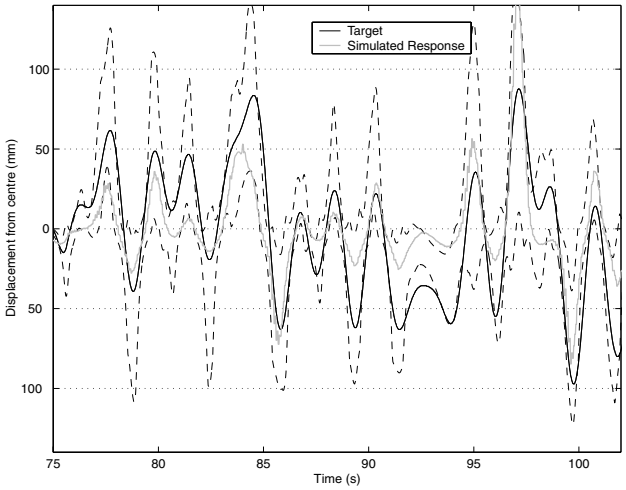

Fig. 6. Simulated open-loop response in relation to the target after 15 runs (static nonlinear system). Dashed lines indicate experimental sd.

the mean experimental response. The simulated trajectory could well represent a typical human response.

B. Static Nonlinear System

The transfer function and coherence plots for the final run are shown in Fig. 5. In closed-loop the simulated gain below 0.5 Hz was higher than observed experimentally. The phase response was very close to the experimental mean, and the simulated coherence exhibited a characteristic drop above 0.4 Hz as seen experimentally.

The open-loop results show the same drop in gain and coherence below 0.3 Hz that was characteristic of the mean experimental results. The gain is lower than the experimental mean across the target bandwidth but remains within one standard deviation of the mean except at very low frequencies.. The simulated drop in coherence is stronger than that observed in the mean human data, with a particularly clear disparity at very low frequency (0 Hz in Fig. 5). The simulated open-loop results show a strong phase lead for frequencies in the lower half of the target bandwidth.

The experimental mean exhibits an approximately linear phase lead to reach 20° at 0.6 Hz. In contrast, in the simulated phase response, a phase lead at low frequencies reverses at higher frequencies, resulting in a slight phase lag from 0.5–0.6 Hz.

Fig. 6 shows the simulated open-loop response trajectory for run 15. The response shows very similar characteristics to the unusual response trajectories observed in the experiment. The simulated trajectory again remains within one standard deviation of the mean experimental response

VI. Discussion

The nAMT computational model succeeded in generating responses which reproduced many of the principle characteristics of the response trajectories obtained during the experimental study. Importantly, these results were obtained using a single set of parameters across the wide range of conditions studied in the experiment (i.e., both closed- and open-loop control and several different external systems). As hoped, the nAMT model was able to suggest a possible cause for the unusual open-loop trajectories.

It proved possible to generate a high-pass gain with a phase lead in the absence of response feedback while retaining acceptably accurate performance in closed-loop (see Fig. 3 and Fig. 5). The ability of the model to achieve these results arose from the inversion method employed in nAMT, the internal feedback loop, which argues in favor of the existence of similar circuitry in the brain [9]. The internal loop-gain found to optimally reproduce the experimental results was found to be surprisingly low ($P = 0.5$, $D = 1$, $I = 0.05$), suggesting a dominant role for feedback control at this target bandwidth (0.6 Hz). It is notable that both FEL and AMT are incapable of reproducing this disparity between closed- and open-loop results without modification to their structures.

It is usually suggested that during learning the inverse model becomes increasingly accurate until final convergence is achieved. In a combined adaptive control structure the open-loop response trajectory would consequently become increasingly similar to the target. There is no obvious reason why only the high frequencies should be learned accurately, as appears to be the case in the experimental results. This is particularly true for a target signal with an approximately flat frequency response like that used in this study.

In simulation, both AMT and FEL behave as predicted: the inverse model becomes increasingly accurate, *particularly* at low frequencies. Indeed, to prevent an accurate inverse model forming at low frequencies an artificial filter needs to be added to deliberately disrupt the model. While such low frequency disruption can be compensated for by the closed-loop controller, and hence would not affect normal performance, it is difficult to suggest why the brain would disrupt the inverse in this manner.

In nAMT, using a low internal feedback loop-gain maximizes the stability of the loop but also essentially filters the motor response. This prevents the inverse from becoming accurate at all frequencies. This inversion method trades inverse model accuracy for stability. Even when the forward model is entirely accurate it may be necessary to keep the loop-gain low to maintain inverse loop stability. Hence, unlike other combined motor models, the nAMT structure could potentially finish learning with a completely accurate forward model but, due to a low loop-gain, retain an inaccurate inverse indefinitely.

The experimentally observed behavior arose from the nAMT structure with no major additions or alterations. This is supportive of the claim that an internal feedback loop is used for the inversion of external systems in the human brain [9]. Paradoxically, the standard AMT model, FEL and, to our knowledge, all other control-systems-type motor control models are incapable of reproducing these results due to the accuracy of the inversion techniques they employ.

VII. References

[1] P. R. Davidson, R. D. Jones, H. R. Sirisena, and J. H. Andreae, "Detection of adaptive inverse models in the human motor system," *Hum. Movement Sci.*, vol. 19, pp. 761-795, 2000.

[2] M. Kawato, Y. Uno, M. Isobe, and R. Suzuki, "Hierarchical neural network model for voluntary movement with application to robotics," in *IEEE Contr. Syst. Mag.*, vol. 8, 1988, pp. 8-16.

[3] M. Kawato and H. Gomi, "A computational model of four regions of the cerebellum based on feedback-error learning," *Biol. Cyber.*, vol. 68, pp. 95-103, 1992.

[4] M. Kawato, K. Furukawa, and R. Suzuki, "A hierarchical neural network model for control and learning of voluntary movement," *Biol. Cyber.*, vol. 57, pp. 169-185, 1987.

[5] P. D. Neilson, M. D. Neilson, and N. J. O'Dwyer, "Adaptive model theory: Application to disorders of motor control," in *Approaches to the study of motor control and learning*, J. J. Summers, Ed. Amsterdam: Elsevier, 1992, pp. 495-548.

[6] P. D. Neilson, M. D. Neilson, and N. J. O'Dwyer, "Adaptive model theory: Central processing in acquisition of skill," in *Neurophysiology and neuropsychology of motor development*, K. J. Connelly and H. Fossberg, Eds. London: MacKeith Press, 1997, pp. 1-43.

[7] R. C. Miall, "The cerebellum and visually controlled movements," presented at IEE Workshop on Self-Learning Robots III: Brain Style Robotics, London, 1999.

[8] R. C. Miall, D. J. Weir, D. M. Wolpert, and J. F. Stein, "Is the cerebellum a Smith predictor?," *J. Motor. Behav.*, vol. 25, pp. 203-216, 1993.

[9] R. C. Miall and D. M. Wolpert, "Forward models for physiological motor control," *Neural Networks*, vol. 9, pp. 1265-1279, 1996.

[10] A. Sriharan, "Mathematical modelling of the human operator control system through tracking tasks," in *Electrical Engineering*. Sydney: University of New South Wales, 1997.

[11] L. Ljung, *System identification: Theory for the user*, 2nd ed. Upper Saddle River, N.J.: Prentice Hall PTR, 1999.